Asian Journal of Chemistry; Vol. 24, No. 7 (2012), 3194-3196

ASIAN JOURNAL OF CHEMISTRY

www.asianjournalofchemistry.co.in

Effects of Hole Etching Depth in a Long Wavelength InGaAsP Photonic Crystal Vertical Cavity Surface Emitting Laser

SAEID MARJANI[1,*] and HAMID MARJANI[2]

[1]Young Researchers Club, Arak Branch, Islamic Azad University, Arak, Iran
[2]Department of Electrical Engineering, Arak Branch, Islamic Azad University, Arak, Iran

*Corresponding author: E-mail: saeidmarjani@yahoo.com

(*Received*: 11 August 2011; *Accepted*: 22 February 2012) AJC-11099

In the present work, we presented the effects of the hole etching depth on various elements of heat sources within the active region of a long-wavelength InGaAsP photonic crystal vertical cavity surface emitting laser. The device employs InGaAsP active region, which is sandwiched between GaAs/AlGaAs and GaAs/AlAs distributed Bragg reflectors (DBRs). This paper provides key results of the various elements of heat sources upon the hole etching depth, including the Joule heat power, the recombination heat power and the Thomson heat power.

Key Words: Hole etching depth, InGaAsP, Photonic crystal, Vertical cavity surface emitting laser.

INTRODUCTION

A crystal is a periodic arrangement of atoms or molecules. The pattern which the atoms or molecules are repeated in space is the crystal lattice. The crystal presents a periodical potential to an electron propagating through it and both the constituents of the crystal and the geometry of the lattice dictate the conduction properties of the crystal. If the dielectric constants of the materials in the crystal are sufficiently different and if the absorption of light by the materials is minimum, then the refractions and reflections of light from all the different interfaces can present many of the same phenomena for photons that the atomic potential produces for electrons.

Fig. 1 is a schematic representation of several three-dimensional lattices of spheres in a cubic cell. The simplest lattice is formed by the blue spheres at the corners of the cube. If we add the dark red spheres at the centers of the faces, we obtain a face-centered cubic (or fcc) lattice. The fcc lattice vectors are (ˆx + ˆy) a/2, (ˆy + ˆz) a/2 and (ˆx + ˆz) a/2. Finally, if we add the pink spheres, which represent another fcc lattice that is shifted by (a/4, a/4, a/4) relative to the blue spheres, then we obtain a diamond lattice[1].

In recent years, the vertical cavity surface emitting lasers have attracted extremely[2]. Vertical cavity surface emitting laser is one of the key light source used in high performance optical communication systems where single mode operation, high output power, high speed modulation and low manufacture cost are necessary[3]. High optical gain in the active area and high thermal conductivity in the reflecting mirrors are the main difficulties in developing vertical cavity surface emitting laserss, which are used in the field of optical spectroscopy[4].

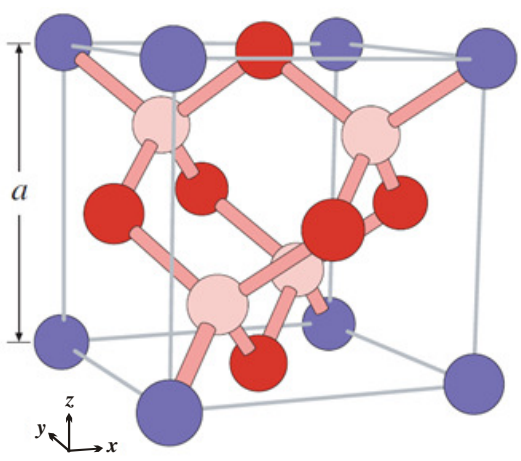

Fig. 1. Ball-and-stick (atomic) representation of several three-dimensional lattices in a cubic supercell, with a lattice constant a. The blue balls alone form a simple cubic lattice. Adding the dark red balls produces a face-centered cubic (fcc) lattice. Adding the pink balls as well produces a diamond lattice, with stick "bonds" (four bonds per ball)

Lattice heat is generated whenever physical processes transfer energy to the crystal lattice. According to differences in transfer mechanisms, heat sources can be separated into

Joule heat, electron-hole recombination heat, Thomson heat and heat from optical absorption. Self-heating often limits the performance of optoelectronic devices. Heat is generated when carriers transfer part of their energy to the crystal lattice. In consequence, the thermal energy of the lattice rises, which is measured as an increase in its temperature[5].

In this paper, we introduced the effects of the hole etching depth on various elements of heat sources within the active region of a photonic crystal vertical cavity surface emitting laser operating in the 1.57 μm wavelength regime. In the following, we first describe the numerical model. Next the simulated photonic crystal vertical cavity surface emitting laser structure is introduced, later we present the results. Finally, the conclusions provide common guidelines for designing performance of photonic crystal vertical cavity surface emitting lasers.

EXPERIMENTAL

In modeling vertical cavity surface emitting laser, we must consider the electrical, optical and thermal interaction during laser performance. Thus base of simulation is to solve Poisson and continuity equations for electrons and holes[6]. Poisson's equation is defined by:

$$\nabla.(\varepsilon\nabla\psi) = \rho \tag{1}$$

where, Ψ is electrostatic potential, ρ is local charge density and ε is local permittivity. The continuity equations of electron and hole are given by[5]:

$$\frac{dn}{dt} = G_n - R_n + \frac{1}{q}\nabla.j_n \tag{2}$$

$$\frac{dp}{dt} = G_p - R_p + \frac{1}{q}\nabla.j_p \tag{3}$$

where, n and p are the electron and hole concentration, J_n and J_p are the electron and hole current densities, G_n and G_p are the generation rates for electrons and holes, R_n and R_p are the recombination rates and q is the magnitude of electron charge.

The fundamental semiconductor equations (1)-(3) are solved self-consistently together with Helmholtz and the photon rate equations. The applied technique for solution of Helmholtz equation is based on improved effective index model[7], which shows accuracy for great portion of preliminary problems. This model is very good adapted to simulation of laser structures and it is often called effective frequency method[8].

Two-dimensional Helmholtz equation is solved to determine the transverse optical field profile and it is given by[6]:

$$\nabla^2 E(r,z,\varphi) + \frac{\omega_0}{c^2}\varepsilon(r,z,\varphi,\omega)E(r,z,\varphi) = 0 \tag{4}$$

where, ω is the frequency, ε(r, z, φ, ω) is the complex dielectric permittivity, E(r, z, φ) is the optical electric field and c is the speed of light in vacuum. The light power equation relates electrical and optical models. The photon rate equation is given by[6]:

$$\frac{dS_m}{dt} = \left(\frac{c}{N_{eff}}G_m - \frac{1}{\tau_{ph_m}} - \frac{cL}{N_{eff}}\right)S_m + R_{sp_m} \tag{5}$$

where, S_m is the photon number, G_m is the modal gain, R_{spm} is the modal spontaneous emission rate, L represents the losses in the laser, N_{eff} is the group effective refractive index, τ_{phm} is the modal photon lifetime and c is the speed of light in vacuum. The heat flow equation has the form[6]:

$$C\frac{\partial T_L}{\partial t} = \nabla(\kappa\nabla T_L) + H \tag{6}$$

where C is the heat capacitance per unit volume, κ is the thermal conductivity, H is the generation, T_L is the local lattice temperature and H is the heat generation term.

The heat generation equation has the form[6]:

$$H = \left[\frac{\left|\overrightarrow{J_n}\right|^2}{q\mu_n n} + \frac{\left|\overrightarrow{J_p}\right|^2}{q\mu_p p}\right] + q(R-G)[\phi_p - \phi_n + T_L(P_p - P_n)] - T_L(\vec{J}_n\nabla P_n + \vec{J}_p\nabla P_p) \tag{7}$$

where, $\left[\frac{\left|\overrightarrow{J_n}\right|^2}{q\mu_n n} + \frac{\left|\overrightarrow{J_p}\right|^2}{q\mu_p p}\right]$ is the Joule heating term, $q(R-G)[\phi_p - \phi_n + T_L(P_p - P_n)]$ is the recombination and generation heating and cooling term, $-T_L(\vec{J}_n\nabla P_n + \vec{J}_p\nabla P_p)$ accounts for the Peltier and Thomson effects.

Equations (1)-(7) provide an approach that can account for the mutual dependence of electrical, thermal, optical and elements of heat sources.

Fig. 2(a) shows the schematic structure of photonic crystal vertical cavity surface emitting laser device, which is used for simulation. The vertical cavity surface emitting laser device consists of an active region of six $In_{0.76}Ga_{0.24}As_{0.82}P_{0.18}$ quantum wells and seven $In_{0.48}Ga_{0.52}As_{0.82}P_{0.18}$ barriers, bounded between 30 periods of top and 28 periods of bottom distributed Bragg reflectors mirrors. The top one is GaAs/$Al_{0.33}Ga_{0.67}As$ with reflection factor of layers 3.38 and 3.05 respectively and the bottom one is GaAs/AlAs with reflection factor of layers 3.38 and 2.89, respectively. The incorporation of a high aluminum content layer ($Al_{0.98}Ga_{0.02}As$) in two distributed Bragg reflectors periods above the active region allows for selective oxidation[9]. Triangular-lattice air holes are formed in the upper pairs of top distributed Bragg reflectors. The optical confinement is achieved by means of seven air holes where the center is missed off to make the defect region, as shown in Fig. 2(b).

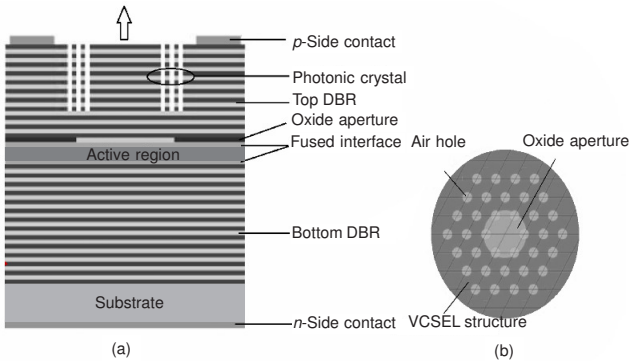

Fig. 2. (a) Schematic structure of the vertical cavity surface emitting laser device and (b) Top view of the triangular-lattice air holes pattern

RESULTS AND DISCUSSION

In the present work, the influence of the hole etching depth on various elements of heat sources is analyzed and discussed.

Fundamentally, the heat power peaks at the MQW region for all heat source elements. The highest contributor of heat power comes from the Peltier-Thomson heat power (up to 2.5e10 W/cm^3) followed by the joule heat power (up to 2.4e9 W/cm^3) and finally the recombination heat power (5.75e8 W/cm^3).

Fig. 3(a) portrays the joule heat power within a vertical cross-section of the active region. As can be seen from Fig. 3(a), increasing of the hole etching depth causes the reduction of the joule heat power. By increasing of the depth into the active region, the peak joule heat power increases. Maximum joule heat power achieved is 2.4e9 W/cm^3 for shallow hole etching (dE = 2 μm).

Fig. 3(b) shows the Peltier- Thomson heat power within a vertical cross-section of the active region while the hole etching depth is changed. It can be found that the increment of the hole etching depth from 2 to 6 μm, leads to the lower Peltier-Thomson heat power.

Figure 3(c) shows the recombination heat power within a vertical cross-section of the active region while the hole etching depth is changed. As shown in the Fig. 3(c), when the hole etching depth increases, the recombination heat power shows the same rule as that at the Peltier-Thomson heat power. However, by increasing the depth into the active region, effect of the hole etching depth decreases on the recombination heat power but totally the peak recombination heat power decreases.

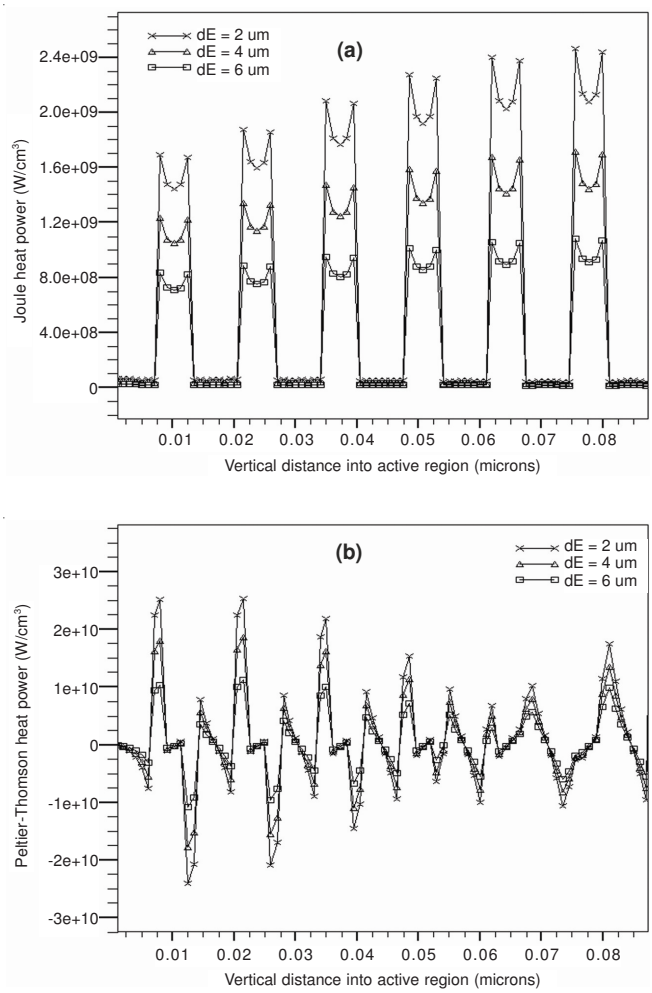

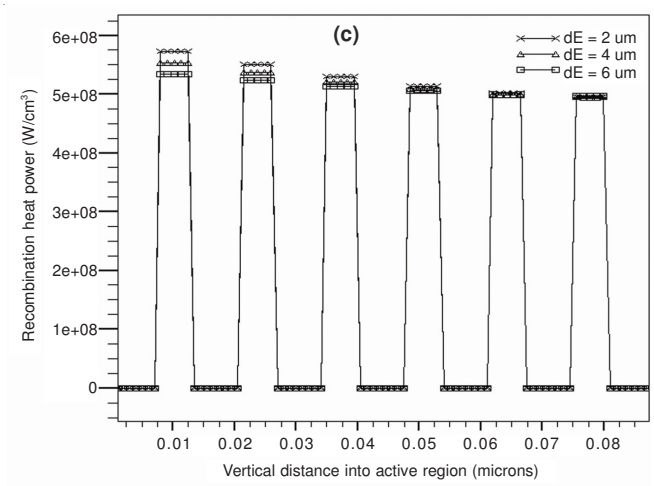

Fig. 3. Effects of the hole etching depth on various elements of heat sources within the active region (a) Joule heat power, (b) Peltier- Thomson heat power and (c) Recombination heat power

Conclusion

In this work, we present the effects of the hole etching depth on various elements of heat sources within the active region of a long wavelength InGaAsP photonic vertical cavity surface emitting laser. The results indicate that increasing of the hole etching depth causes the reduction of all heat source elements into MQW region. Simulation results show that the highest contributor of heat power comes from the Peltier-Thomson heat power (up to 2.5e10 W/cm^3) followed by the joule heat power (up to 2.4e9 W/cm^3) and finally, the recombination heat power (5.75e8 W/cm^3). This paper provided an approach that can account for the mutual dependence of the hole etching depth, thermal resistance and the elements of heat sources.

REFERENCES

1. J.D. Joannopoulos, S.G. Johnson, R.D. Meade and J.N. Winn, Photonic Crystals: Molding the Flow of Light, Princeton, Univ. Press, edn. 2, pp. 94-99 (2008).
2. K. Iga, *J. IEEE Select. Topics Electron*, **6**, 1201 (2000).
3. M. Dems, R. Kotynski and K. Panajotov, *J. Opt. Express*, **13**, 3196 (2005).
4. E. Kapon and A. Sirbu, *J. Nat. Photonics*, **3**, 27 (2009).
5. J. Piprek, Semiconductor Optoelectronic Devices: Introduction to Physics and Simulation, Ch. 3 Carrier Transport and Ch. 6 Heat Generation and Dissipation UCSB: Academic Press, pp. 49-50 and pp. 141-147 (2003).
6. Silvaco International, Atlac User's Manual, USA, Silvaco International Incorporated (2010).
7. G.R. Hadley, *J. Opt. Lett.*, **20**, 1483 (1995).
8. H. Wenzel and H.J. Wunsche, *IEEE J. Quantum Electron.*, **33**, 1156 (1997).
9. K.D. Choquette, K.M. Geib, C.I. Ashby, R.D. Twesten, O. Blum, H.Q. Hou, D.M. Follstaedt, B.E. Hammons, D. Mathes and R. Hull, *IEEE J. Sel. Topics Quantum Electron.*, **3**, 916 (1997).